Purification and Characterization from Rat Liver Cytosol of a GDP Dissociation Inhibitor (GDI) for Liver 24K G, a *ras* p21-like GTP-Binding Protein, with Properties Similar to Those of *smg* p25A GDI†

Takashi Ueda,‡ Yoshifumi Takeyama,*,‡ Toshihiko Ohmori,‡ Harumasa Ohyanagi,‡ Yoichi Saitoh,‡ and Yoshimi Takai§

Departments of Surgery (1st Division) and Biochemistry, Kobe University School of Medicine, Kobe 650, Japan
Received July 6, 1990; Revised Manuscript Received September 18, 1990

ABSTRACT: A regulatory protein for a liver GTP-binding protein (G protein) with a molecular weight value of 24000 (24K G), which we have recently purified, was purified to near-homogeneity from rat liver cytosol and characterized. This regulatory protein, designated here as GDP dissociation inhibitor for 24K G (24K G GDI), inhibited the dissociation of GDP from and the subsequent binding of GTP to 24K G. 24K G GDI was inactive for other *ras* p21/*ras* p21-like small G proteins including c-Ha-*ras* p21, *rho*B p20, *smg* p21B, and *smg* p25A. 24K G was, however, recognized by bovine brain *smg* p25A GDI which regulated the GDP/GTP exchange reaction of *smg* p25A. By analyses of sodium dodecyl sulfate (SDS)–polyacrylamide gel electrophoresis (PAGE), immunoblotting with anti-*smg* p25A GDI antibody, two-dimensional PAGE, and C_4 column chromatography, 24K G GDI showed physical properties very similar to those of *smg* p25A GDI. The peptide map and the partial amino acid sequences of 24K G GDI were not identical with those of *smg* p25A GDI. Among the 83 residues, 2 amino acids were different between rat liver 24K G GDI and bovine brain *smg* p25A GDI. These results indicate that there is a specific regulatory protein for 24K G, 24K G GDI, in rat liver cytosol and that 24K G GDI has close similarity to *smg* p25A GDI.

Liver synthesizes the majority of the plasma proteins and secretes them in the constitutive pathway. Under certain pathological conditions of liver, hyposynthesis and/or inappropriate secretion of the plasma proteins such as albumin are observed and develop the malfunctions of other organs. The intracellular traffic of proteins in hepatocytes is considered to be interfered at some steps under such conditions. It is important to clarify the molecular mechanisms of the intracellular vesicular traffic in liver.

It is strongly suggested that small G proteins[1] are involved in the regulation of the secretory pathways in mammalian cells [for reviews, see Gomperts (1986), Burgoyne (1987), and Bourne (1988)]. In addition, in yeast it has been demonstrated that the *YPT1* (Segev et al., 1988) and *SEC4* (Salminen & Novick, 1987; Goud et al., 1988) proteins are involved in the secretory processes. We have shown that *smg* p25A [the bovine counterpart of the rat *rab*3 protein (Kikuchi et al., 1988; Matsui et al., 1988; Zahraoui et al., 1988)] is detected in specialized secretory cells such as exocrine, endocrine, and neuronal cells (Kim et al., 1989; Mizoguchi et al., 1989, 1990). Therefore, it is likely that small G proteins are implicated in the intracellular vesicular traffic in liver.

Though small G proteins purified from liver had not been reported, we have separated at least six G proteins from the microsomes–Golgi complex fraction of rat liver in a preceding paper (Ohmori et al., 1990). Among these six G proteins, we have purified a G protein with a molecular weight value of 24000 (24K G) to near-homogeneity and characterized it. Analysis of the partial amino acid sequences of 24K G has revealed that this G protein is a novel member of the superfamily of *ras* p21/*ras* p21-like small G proteins [for reviews, see Barbacid (1987) and Takai et al. (1988)]. The function of 24K G in liver is unknown at present, but 24K G may be implicated in the intracellular vesicular traffic in liver.

The modes of activation and action of small G proteins have been extensively analyzed. By analogy with *ras* p21, it is conceivable that small G proteins have the GDP-bound inactive form and the GTP-bound active form and that there are proteins converting the inactive form to the active form and an effector protein whose function is modulated by the active form. Consistently, it has been shown that there are at least three types of regulatory proteins for some small G proteins. The first type of regulatory protein, designated as GTPase activating protein (GAP), stimulates the GTPase activity of each small G protein without affecting the GDP/GTP exchange reaction. *ras* p21 GAP (Trahey & McCormick, 1987; Gibbs et al., 1988; Vogel et al., 1988; Trahey et al., 1988), *smg* p21 GAPs (Ueda et al., 1989; Kikuchi et al., 1989), and *rho* GAP (Garrett et al., 1989; Yamamoto, J., et al., 1990) have been purified. The second type of regulatory protein,

† The investigation in the Department of Surgery (1st Division) was supported by Grants-in-Aid for Scientific Research from the Ministry of Education, Science, and Culture, Japan (1989). The investigation in the Department of Biochemistry was supported by Grants-in-Aid for Scientific Research and Cancer Research from the Ministry of Education, Science, and Culture, Japan (1989), Grants-in-Aid for Abnormalities in Hormone Receptor Mechanisms, Cardiovascular Disease, and for Cancer Research from the Ministry of Health and Welfare, Japan (1989), and by grants from the Yamanouchi Foundation for Research on Metabolic Disease (1989) and the Research Program on Cell Calcium Signal in the Cardiovascular System (1989).
* To whom correspondence should be addressed.
‡ Department of Surgery (1st Division).
§ Department of Biochemistry.

[1] Abbreviations: G proteins, GTP-binding proteins; GAP, GTPase activating protein; GDI, GDP dissociation inhibitor; GDS, GDP dissociation stimulator; GTPγS, guanosine 5′-*O*-(3-thiotriphosphate); API, *Achromobacter* protease I; SDS, sodium dodecyl sulfate; PAGE, polyacrylamide gel electrophoresis; BSA, bovine serum albumin; EGTA, [ethylenebis(oxyethylenenitrilo)]tetraacetic acid; DTT, dithiothreitol; ER, endoplasmic reticulum; p*I*, isoelectric point.

0006-2960/91/0430-909$02.50/0

designated as GDP dissociation inhibitor (GDI), inhibits the dissociation of GDP from and the subsequent binding of GTP to each small G protein without affecting the GTPase activity. *smg* p25A GDI (Sasaki et al., 1990) and *rho* GDI (Ohga et al., 1989; Ueda et al., 1990) have been purified and their cDNAs have been cloned (Matsui et al., 1990; Fukumoto et al., 1990). The third type of regulatory protein, designated as GDP dissociation stimulator (GDS), stimulates the dissociation of GDP from and the subsequent binding of GTP to each small G protein without affecting the GTPase activity. We have recently purified *smg* p21s GDSs (Yamamoto, T., et al., 1990) and *rho* GDSs (Isomura et al., 1990). The *CDC25* protein has been also suggested to serve as a stimulatory regulatory protein for the GDP/GTP exchange reaction of the *RAS* protein in yeast (Broek et al., 1987). The activity to stimulate the GDP/GTP exchange reaction of *ras* p21 has recently been detected in bovine and rat brain (West et al., 1990; Wolfman & Macara, 1990). In the case of vesicular transport, a small G protein(s) functioning in this system may be also regulated by these regulatory proteins. Therefore, it is important to identify a regulatory protein(s) for each small G protein and to characterize its (their) properties for understanding its (their) modes of action in the regulation of the activity of each small G protein in the secretory pathways.

In the present studies, to clarify the mechanism for the regulation of 24K G activity, we have attempted to identify a regulatory protein(s) for 24K G. We have detected the GDI activity for 24K G but not the GAP or GDS activity for it in the cytosol fraction of rat liver. We have purified the GDI for 24K G (24K G GDI) to near-homogeneity from this fraction and characterized it. Moreover, we have found that bovine brain *smg* p25A GDI is active for 24K G as well as *smg* p25A and that rat liver 24K G GDI is similar to bovine brain *smg* p25A GDI.

Experimental Procedures

Materials and Chemicals. Adult male rats (200–250-g weight) of a Sprague-Dawley strain were employed. 24K G was purified from the microsomes–Golgi complex fraction of rat liver (Ohmori et al., 1990). *smg* p25A GDI and *rho* GDI were purified to near-homogeneity from bovine brain cytosol (Sasaki et al., 1990; Ueda et al., 1990). *smg* p25A and *rho*B p20 were purified from bovine brain membranes (Kikuchi et al., 1988; Yamamoto et al., (1988). *smg* p21B was purified from human platelet membranes (Ohmori et al., 1989). c-Ha-*ras* p21 was purified from human c-Ha-*ras* p21 expressing *Escherichia coli*, a gift from Drs. Y. Kaziro and T. Satoh (University of Tokyo, Tokyo, Japan), as described (Satoh et al., 1988). [^{3}H]GDP (specific activity, 42.9 GBq/mmol) and [γ-^{32}P]GTP (specific activity, 370 GBq/mmol) were from Amersham Corp. [^{35}S]GTPγS (specific activity, 48.8 TBq/mmol) was from Du Pont–New England Nuclear. Nitrocellulose filters, Advantec A045A304D with 0.45-μm pore size and S&S BA-85 with the same pore size, were obtained from Toyo Roshi Co. (Tokyo, Japan) and Schleicher & Schuell, respectively. DEAE-Sephacel, Mono Q HR10/10, and Mono Q HR5/5 were obtained from Pharmacia LKB Biotechnology, Inc. An anti-*smg* p25A GDI monoclonal antibody and an anti-*rho* GDI monoclonal antibody were made by immunizing mice with *smg* p25A GDI and *rho* GDI purified from bovine brain cytosol, respectively.[2] A YMC pack AP-802 C_4 column (4.6 × 150 mm) and a Bakerbond WP C_8 column (4.6 × 250 mm) were purchased from Yamamura Chemical Lab Co. (Kyoto, Japan) and J. T. Baker Chemical Co., respectively. API was from Wako Pure Chemical Industries, Ltd. (Osaka, Japan). Other materials and chemicals were obtained from commercial sources.

Assay for 24K G GDI during the Purification Procedures (Method 1). 24K G GDI was assayed by the rapid filtration method as described (Ueda et al., 1990). Neither the [^{3}H]-GDP- nor the [^{35}S]GTPγS-bound form of 24K G passed through Advantec A045A304D nitrocellulose filters. 24K G GDI, however, made the [^{3}H]GDP-bound form, but not the [^{35}S]GTPγS-bound form, of 24K G pass through this type of filter in a dose-dependent manner, although the reason for this phenomenon is not known. Since 24K G GDI did not stimulate the dissociation of [^{3}H]GDP from 24K G as described below, 24K G GDI could be quantified by measuring the decrease in the radioactivity of the [^{3}H]GDP-bound form of 24K G trapped on this type of filter. The [^{3}H]GDP-bound form of 24K G was first made by incubating 24K G (50 ng of protein) with [^{3}H]GDP at 0.5 μM Mg^{2+} for 20 min at 30 °C in a 25-μL mixture. Then the assay sample of 24K G GDI was added, and the second incubation was performed at 10 mM Mg^{2+} for 10 min at 4 °C in a 100-μL mixture followed by rapid filtration through Advantec A045A304D nitrocellulose filters. Method 1 was usually used during the purification procedures.

Assay for the Dissociation of [^{3}H]GDP from 24K G (Method 2). Since the [^{3}H]GDP-bound form of 24K G was trapped on S&S BA-85 nitrocellulose filters irrespective of the presence of 24K G GDI, the dissociation of [^{3}H]GDP from 24K G was assayed by use of this type of filter as described (Ueda et al., 1990). After the [^{3}H]GDP-bound form of 24K G was made as described under Method 1, the assay sample of 24K G GDI was added, and the second incubation was performed at 5 mM Mg^{2+} for 5 min at 30 °C. Then the dissociation of [^{3}H]GDP from 24K G in the presence or absence of 24K G GDI was assayed at 0.5 μM or 10 mM Mg^{2+} for the indicated periods at 30 °C in a 100-μL mixture, and the inhibitory activity of 24K G GDI in this dissociation was measured.

Assay for the Binding of [^{35}S]GTPγS to the GDP-Bound Form of 24K G (Method 3). Since the [^{35}S]GTPγS-bound form of 24K G was trapped on S&S BA-85 nitrocellulose filters irrespective of the presence of 24K G GDI, the binding of [^{35}S]GTPγS to 24K G was assayed by use of this type of filter as described (Ueda et al., 1990). After the GDP-bound form of 24K G was made by nonradioactive GDP, the assay sample of 24K G GDI was added, and the second incubation was performed as described under Method 2. Then the binding of [^{35}S]GTPγS to this form in the presence or absence of 24K G GDI was assayed at 0.5 μM or 10 mM Mg^{2+} for the indicated periods at 30 °C in a 100-μL mixture, and the inhibitory activity of 24K G GDI in this binding was measured.

YMC Pack AP-802 C_4 Column Chromatography. The purified 24K G GDI and *smg* p25A GDI (2 μg of each protein) were applied to a YMC pack AP-802 C_4 column preequilibrated with 0.1% trifluoroacetic acid. The elution was performed with a 40-mL linear gradient of acetonitrile–2-propanol (0–100%, acetonitrile:2-propanol ratio = 3:7) in 0.1% trifluoroacetic acid at a flow rate of 1 mL/min.

Analyses of Peptide Map and Amino Acid Sequences. 24K G GDI and *smg* p25A GDI (13 μg of each protein) prepared by a YMC Pack AP-802 C_4 column as described above were digested with API at a molar ratio of 1:100 (API:each sample) for 18 h at 37 °C in 200 μL of 200 mM Tris-HCl at pH 9.0.

[2] The detailed procedures for the generation of these antibodies and their properties will be described elsewhere.

The API-digested peptides were applied to a Bakerbond WP C_8 column preequilibrated with 0.1% trifluoroacetic acid. The elution was performed with a 60-mL linear gradient of acetonitrile (0–60%) in 0.1% trifluoroacetic acid at a flow rate of 1 mL/min. The peptides separated by this column chromatography were sequenced with an automated gas-phase sequencer (Applied Biosystems, Model 470A).

Other Assays. The GAP activity for 24K G was measured with the [γ-^{32}P]GTP-bound form of 24K G as substrate as described (Ueda et al., 1989). The GDS activity for 24K G was measured as described (Isomura et al., 1990; Yamamoto, T., et al., 1990). Immunoblotting was performed as described (Mizoguchi et al., 1989).

Determinations. The radioactivities of ^{3}H-, ^{35}S-, and ^{32}P-labeled samples were determined by using a liquid scintillation system (Beckman, Model LS 3801). The molecular weight value of 24K G GDI was estimated by SDS–PAGE and sucrose density gradient ultracentrifugation as described (Laemmli, 1970; Martin & Ames, 1961). The p*I* of 24K G GDI was estimated by one- and two-dimensional PAGE (O'Farrell, 1975). Protein concentrations were determined with BSA as a reference protein as described (Bradford, 1976).

Results

Purification of 24K G GDI

Assays for 24K G GDI during the Purification Procedures. The purified 24K G GDI showed three activities: (1) the activity making the GDP-bound form of 24K G pass through the Advantec A045A304D nitrocellulose filters; (2) the activity inhibiting the dissociation of [^{3}H]GDP from 24K G; and (3) the activity inhibiting the binding of [^{35}S]GTPγS to the GDP-bound form of 24K G. These three activities could be measured quantitatively by methods 1–3, respectively. The sensitivity of method 1 was, however, the highest, and those of methods 2 and 3 were the same. Moreover, the 24K G GDI activity of each fraction of the used column chromatographies could not be measured by method 2 unless each fraction was concentrated and dialyzed to remove the detergent. The activity of crude 24K G GDI contaminated by G proteins could not be measured by method 3. Therefore, method 1 was usually used during the following purification procedures.

Preparation of the Cytosol Fraction and DEAE-Sephacel Column Chromatography. All the purification procedures were carried out at 0–4 °C. Ten rats were starved for about 14 h. Livers (60 g, wet weight) were homogenized by three strokes with a Potter–Elvehjem Teflon–glass homogenizer in 240 mL of buffer A (25 mM Tris-HCl at pH 7.5, 1 mM $MgCl_2$, 1 mM EGTA, and 1 mM DTT) containing 10 μM (*p*-amidinophenyl)methanesulfonyl fluoride. The homogenate was centrifuged at 100000*g* for 60 min, and the supernatant (230 mL, 4.1 g of protein) was used as the cytosol fraction. In the cytosol fraction, the GDI activity for 24K G was detected, but neither the GAP activity nor the GDS activity for 24K G was detected (data not shown). The cytosol fraction was applied to a DEAE-Sephacel column (7.5 × 18 cm) equilibrated with buffer A. After the column was washed with 8 L of buffer A and 400 mL of buffer A containing 0.3 M NaCl, 24K G GDI was eluted by 800 mL of buffer A containing 0.3 M NaCl.

Ammonium Sulfate Fractionation. Solid ammonium sulfate was added to this eluate (800 mL, 1.5 g of protein) to give a final concentration of 40% saturation. The sample was centrifuged at 20000*g* for 20 min. 24K G GDI was recovered in the supernatant. Solid ammonium sulfate was further added to the supernatant to give a final concentration of 60% saturation. The sample was centrifuged at 20000*g* for 20 min. All 24K G GDI was precipitated. The 40–60% precipitate was dissolved in 13 mL of buffer B (25 mM Tris-HCl at pH 7.5, 0.5 mM EDTA, and 1 mM DTT). After dialysis against the same buffer, the dialyzed sample was centrifuged at 100000*g* for 60 min. The volume of the supernatant was adjusted to 16 mL by the addition of buffer B.

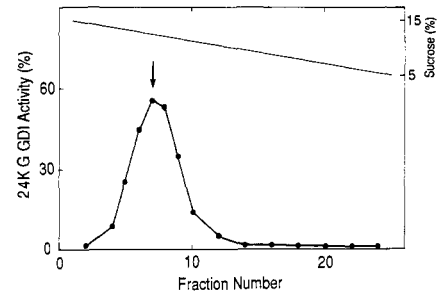

FIGURE 1: Sucrose density gradient ultracentrifugation. Seventy-microliter aliquots of the indicated fractions were used for 24K G GDI assay by method 1. The 24K G GDI activity measured by this method was calculated from the radioactivity of 24K G trapped on the nitrocellulose filters in the presence and absence of 24K G GDI. 24K G GDI activity was expressed as percent decrease in [^{3}H]-GDP-bound 24K G trapped on the nitrocellulose filters. (●) 24K G GDI activity; (—) sucrose concentration. An arrow indicates the position of hemoglobin (M_r 64 500, 4.5 S). The results shown are representative of three independent experiments.

Mono Q Column Chromatography. Half of the supernatant (8 mL, 245 mg of protein) was supplemented with 2.7 mL of buffer B containing 4% sodium cholate. The sample was adjusted to pH 8.0 by 1.5 M Tris and applied to a Mono Q column (1 × 10 cm) equilibrated with buffer B containing 1% sodium cholate. After the column was washed with 190 mL of the same buffer, the elution was performed with a 180-mL linear gradient of NaCl (0–0.5 M) in the same buffer at a flow rate of 2 mL/min. Fractions of 4 mL each were collected. With a 70-μL aliquot of each fraction, which was the maximum volume used for method 1, 24K G GDI activity could not be detected in any fraction by this method. Therefore, the passed-through/first-washed fractions (fractions 1–7), the second-washed fractions (fractions 8–14), the third-washed fractions (fractions 15–32), the fourth-washed fractions (fractions 33–50), and the eluted fractions (fractions 51–95) were collected and then concentrated to approximately 2 mL by an Amicon ultrafiltration cell equipped with a PM-10 filter. After these concentrates were dialyzed against buffer B to decrease the concentration of sodium cholate, 24K G GDI activity was again assayed by method 1. By this approach, most of 24K G GDI activity could be detected in the concentrate of the third-washed fractions.[3] The rest of the 40–60% ammonium sulfate fractionated sample was treated in the same way.

Sucrose Density Gradient Ultracentrifugation. Half of the concentrate (1 mL, 750 μg of protein) of 24K G GDI of one Mono Q column chromatography was subjected to sucrose density gradient ultracentrifugation using five tubes. Each tube contained a 4.8-mL sucrose density gradient (5–15% sucrose in buffer B). Centrifugation was performed at 238000*g* for 19 h. Fractions of 0.2 mL each were collected from the bottom of each tube. 24K G GDI appeared in fractions 6–9 as a single peak (Figure 1). The active fractions of 24K G GDI (4 mL, 215 μg of protein) were collected from five tubes. The rest of the concentrate of one Mono Q column

[3] 24K G GDI was eluted in the second-washed fractions when chromatography was performed with the Mono Q column used several times.

Table I: Purification of 24K G GDI

purification step	total volume (mL)	total protein (mg)	total act. (units)[a]	sp act. (units/mg)	yield (%)
cytosol	230	4100	32000	7.8	100
DEAE-Sephacel	800	1500	17000	11	53
40–60% ammonium sulfate precipitate	16	490	7200	15	23
Mono Q HR10/10	4.0	3.0	2800	930	8.8
sucrose density gradient ultracentrifugation	16	0.86	1300	1500	4.1
second Mono Q HR5/5	6.0	0.12	900	7500	2.8

[a] One unit of the 24K G GDI activity was defined as the amount of 24K G GDI which made 1 pmol of the [^{3}H]GDP-bound form of 24K G pass through the nitrocellulose filters under the standard assay conditions of method 1.

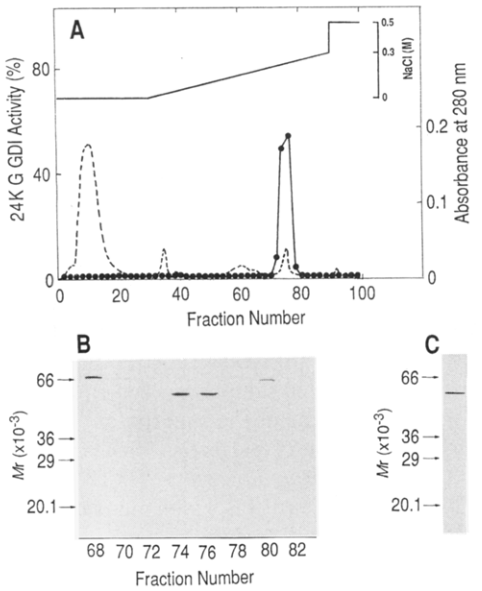

FIGURE 2: Second Mono Q column chromatography and analysis of 24K G GDI on SDS–PAGE. Seventy- and twenty-microliter aliquots of the indicated fractions were used for 24K G GDI assay by method 1 and SDS–PAGE (12% polyacrylamide gel), respectively. (A) Elution profile of 24K G GDI. The 24K G GDI activity was calculated and expressed as described in the legend to Figure 1. (●) 24K G GDI activity; (---) absorbance at 280 nm; (—) NaCl concentration. (B) Protein staining with Coomassie Brilliant Blue. The protein markers used were BSA (M_r 66 000), glyceraldehyde-3-phosphate dehydrogenase (M_r 36 000), carbonic anhydrase (M_r 29 000), and trypsin inhibitor (M_r 20 100). (C) Analysis of 24K G GDI on SDS–PAGE. 24K G GDI (500 ng of protein) was subjected to SDS–PAGE (8–16% polyacrylamide gel), and the protein was visualized with Coomassie Brilliant Blue. The protein markers used were the same as those used in (B). The results shown are representative of three independent experiments.

chromatography and the sample of the other Mono Q column chromatography were treated in the same way.

Second Mono Q Column Chromatography. The samples of 24K G GDI collected from five tubes of one sucrose density gradient ultracentrifugation were mixed together and applied to a Mono Q column (0.5 × 5 cm) equilibrated with buffer B. After the column was washed with 11 mL of the same buffer, the elution was performed with a 30-mL linear gradient of NaCl (0–0.3 M) in the same buffer. The linear gradient was followed by further elution with 5 mL of 0.5 M NaCl in the same buffer. The elution was performed at a flow rate of 0.5 mL/min. Fractions of 0.5 mL each were collected. 24K G GDI appeared in fractions 74–76 as a single peak (Figure 2A). Figure 2B shows the protein staining pattern of the indicated fractions on an SDS–polyacrylamide gel. 24K G GDI was apparently pure. The active fractions (1.5 mL, 30 μg of protein) were collected and used as a purified sample of 24K G GDI. The samples of the other three sucrose density gradient ultracentrifugations were treated in the same way. The summary of the purification of 24K G GDI is shown in Table I.

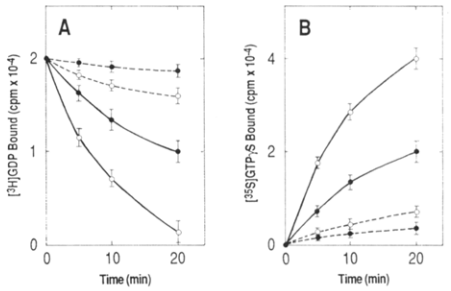

FIGURE 3: Effect of 24K G GDI on the dissociation of [^{3}H]GDP from and the binding of [^{35}S]GTPγS to 24K G. (A) Effect of 24K G GDI on the dissociation of [^{3}H]GDP from 24K G. The assay was performed by method 2 in the presence or absence of 24K G GDI (1 μg of protein) at 0.5 μM Mg^{2+} or 10 mM Mg^{2+}. (—) At 0.5 μM Mg^{2+}; (---) at 10 mM Mg^{2+}; (●) in the presence of 24K G GDI; (○) in the absence of 24K G GDI. (B) Effect of 24K G GDI on the binding of [^{35}S]-GTPγS to the GDP-bound form of 24K G. The assay was performed by method 3 in the presence or absence of 24K G GDI (1 μg of protein) at 0.5 μM Mg^{2+} or 10 mM Mg^{2+}. The symbols are the same as those used in (A). The results shown are the means ± SE of three independent experiments. The background values of [^{35}S]GTPγS binding to the filter in the presence and absence of 24K G GDI without 24K G were 150 and 160 cpm, respectively. The background value was subtracted from each experimental value.

Characterization of 24K G GDI

Molecular Weight Value of 24K G GDI. When the purified preparation of 24K G GDI was subjected to SDS–PAGE and the protein was stained with Coomassie Brilliant Blue, only a single band was observed (Figure 2C). The molecular weight value of this band was estimated to be about 54 000. The S value of 24K G GDI was estimated to be about 4.5 S by sucrose density gradient ultracentrifugation. This value corresponded to a molecular weight value of 65 000.

Effect of 24K G GDI on the Dissociation of [^{3}H]GDP from and the Binding of [^{35}S]GTPγS to 24K G. The initial velocity for the dissociation of [^{3}H]GDP from 24K G was faster at 0.5 μM Mg^{2+} than at 10 mM Mg^{2+} (Figure 3A) as described for other small G proteins (Hall & Self, 1986; Hoshino et al., 1987; Shoji et al., 1989; Kuroda et al., 1989). 24K G GDI inhibited this dissociation at both Mg^{2+} concentrations (Figure 3A). The rate constants of the dissociation of [^{3}H]GDP from 24K G in the absence and presence of 24K G GDI at 0.5 μM Mg^{2+} were about 0.10 and 0.039 min^{-1}, respectively, and those at 10 mM Mg^{2+} were about 0.0099 and 0.0042 min^{-1}, respectively. This inhibitory action of 24K G GDI was eliminated by tryptic digestion or boiling (data not shown).

The initial velocity for the binding of [^{35}S]GTPγS to the GDP-bound form of 24K G was faster at 0.5 μM Mg^{2+} than at 10 mM Mg^{2+} (Figure 3B) as described for other small G proteins (Hall & Self, 1986; Hoshino et al., 1987; Shoji et al., 1989; Kuroda et al., 1989). 24K G GDI inhibited this binding at both Mg^{2+} concentrations (Figure 3B). This inhibitory action of 24K G GDI was eliminated by tryptic digestion or boiling (data not shown).

The two activities of 24K G GDI for inhibiting the dissociation of [^{3}H]GDP from and the binding of [^{35}S]GTPγS to

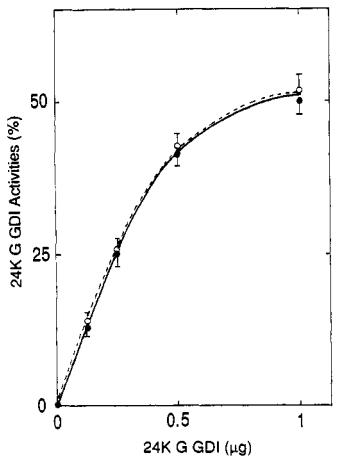

FIGURE 4: Dose-dependent effect of 24K G GDI on the dissociation of [^{3}H]GDP from and the binding of [^{35}S]GTPγS to 24K G. The assays were performed by methods 2 and 3 with the indicated doses of 24K G GDI at 0.5 μM Mg^{2+} for 20 min. The 24K G GDI activities measured by methods 2 and 3 were calculated from the radioactivities of 24K G trapped on the nitrocellulose filters in the presence and absence of 24K G GDI. The 24K G GDI activities measured by methods 2 and 3 were expressed as percent inhibition of the dissociation of [^{3}H]GDP from and the binding of [^{35}S]GTPγS to 24K G, respectively. (●—●) 24K G GDI activity measured by method 2; (○---○) 24K G GDI activity measured by method 3. The results shown are the means ± SE of three independent experiments.

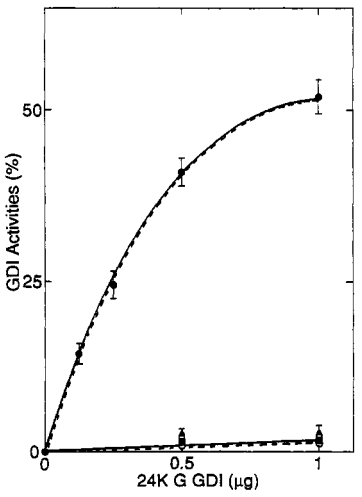

FIGURE 5: Specificity of 24K G GDI for *ras* p21/*ras* p21-like G proteins. The GDI activities of 24K G GDI for 24K G, c-Ha-*ras* p21, *rho*B p20, *smg* p21B, and *smg* p25A were assayed by methods 2 and 3 with the indicated doses of 24K G GDI. Fifty nanograms each of *ras* p21/*ras* p21-like G proteins was used. The assays were performed at 0.5 μM Mg^{2+} for 20 min. The 24K G GDI activities measured by methods 2 and 3 were calculated and expressed as described in the legend to Figure 4. (—) 24K G GDI activities measured by method 2; (---) 24K G GDI activities measured by method 3; (●) for 24K G; (○) for c-Ha-*ras* p21; (■) for *rho*B p20; (□) for *smg* p21B; (▲) for *smg* p25A. The results shown are the means ± SE of three independent experiments.

24K G were dose-dependent, and the doses necessary for these activities were the same (Figure 4). When more than 1 μg of 24K G GDI was used, the dose response curve reached a plateau, so the maximum activities of 24K G GDI were obtained when about 20-fold more 24K G GDI than 24K G was used.

Specificity of 24K G GDI for ras p21/ras p21-like G Proteins. 24K G GDI was inactive for c-Ha-*ras* p21, rhoB p20, *smg* p21B, and *smg* p25A in inhibiting the dissociation of [^{3}H]GDP from and the binding of [^{35}S]GTPγS to each G protein (Figure 5).

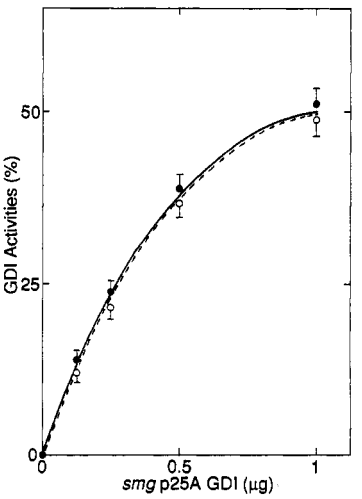

FIGURE 6: GDI activities of *smg* p25A GDI for 24K G and *smg* p25A. Effect of *smg* p25A GDI on the dissociation of [^{3}H]GDP from and the binding of [^{35}S]GTPγS to 24K G and *smg* p25A was assayed by methods 2 and 3 with the indicated doses of *smg* p25A GDI. Fifty nanograms each of 24K G and *smg* p25A was used. The assays were performed at 0.5 μM Mg^{2+} for 20 min. The *smg* p25A GDI activities measured by methods 2 and 3 were calculated and expressed as described in the legend to Figure 4. (—) *smg* p25A GDI activities measured by method 2; (---) *smg* p25A GDI activities measured by method 3; (●) for 24K G; (○) for *smg* p25A. The results shown are the means ± SE of three independent experiments.

Other Properties. 24K G GDI lacked GAP activity for 24K G, c-Ha-*ras* p21, *rho*B p20, *smg* p21B, and *smg* p25A (data not shown). 24K G GDI by itself showed neither [^{35}S]-GTPγS-binding nor GTPase activity (data not shown).

Comparison of the Properties between Rat Liver 24K G GDI and Bovine Brain smg p25A GDI

GDI Activities. We examined the effect of *smg* p25A GDI and *rho* GDI, the GDI type of regulatory proteins thus far purified, for 24K G. *rho* GDI was inactive for 24K G (data not shown), but *smg* p25A GDI inhibited the dissociation of [^{3}H]GDP from and the binding of [^{35}S]GTPγS to 24K G as well as *smg* p25A in a dose-dependent manner (Figure 6). Moreover, *smg* p25A GDI purified from *Escherichia coli* also showed the GDI activities for 24K G as well as *smg* p25A (data not shown). The inhibitory actions of *smg* p25A GDI for *smg* p25A were not affected by the addition of 24K G GDI (data not shown). When about 10-fold more *smg* p25A than 24K G was used, 24K G GDI was inactive for *smg* p25A under the conditions where the maximum activity of 24K G GDI for 24K G was observed (data not shown). These results indicate that 24K G GDI is specific for 24K G, but *smg* p25A GDI is active not only for *smg* p25A but also for 24K G.

SDS–PAGE Analysis. Rat liver 24K G GDI and bovine brain *smg* p25A GDI were subjected to SDS–PAGE either separately or as a mixture. On this SDS–PAGE, both proteins migrated as a single band at the same position (Figure 7A). The molecular weight values of both proteins were estimated to be about 54 000.

Immunoblot Analysis of 24K G GDI. When rat liver 24K G GDI was immunoblotted with the anti-*smg* p25A GDI monoclonal antibody, rat liver 24K G GDI as well as bovine brain *smg* p25A GDI was recognized by this monoclonal antibody (Figure 7B). *rho* GDI was not recognized by this anti-*smg* p25A GDI antibody (data not shown). Neither 24K G GDI nor *smg* p25A GDI was recognized by an anti-*rho* GDI monoclonal antibody (data not shown).

Two-Dimensional PAGE Analysis. Rat liver 24K G GDI and bovine brain *smg* p25A GDI were subjected to O'Farrell's

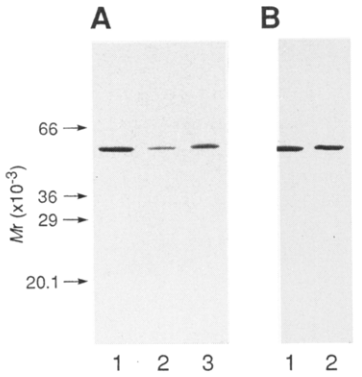

FIGURE 7: Protein staining and immunoblotting of rat liver 24K G GDI and bovine brain *smg* p25A GDI. (A) Protein staining. 24K G GDI and *smg* p25A GDI were subjected to SDS–PAGE (8–16% polyacrylamide gel) followed by protein staining with Coomassie Brilliant Blue. Lane 1, 24K G GDI (500 ng of protein) plus *smg* p25A GDI (500 ng of protein); lane 2, 24K G GDI (500 ng of protein); lane 3, *smg* p25A GDI (500 ng of protein). (B) Immunoblotting with anti-*smg* p25A GDI antibody. 24K G GDI and *smg* p25A GDI (200 ng of each protein) were subjected to SDS–PAGE, transferred electrophoretically from the gel to a nitrocellulose sheet, and reacted with anti-*smg* p25A GDI monoclonal antibody. Lane 1, 24K G GDI; lane 2, *smg* p25A GDI. The protein markers used were the same as those used in Figure 2.

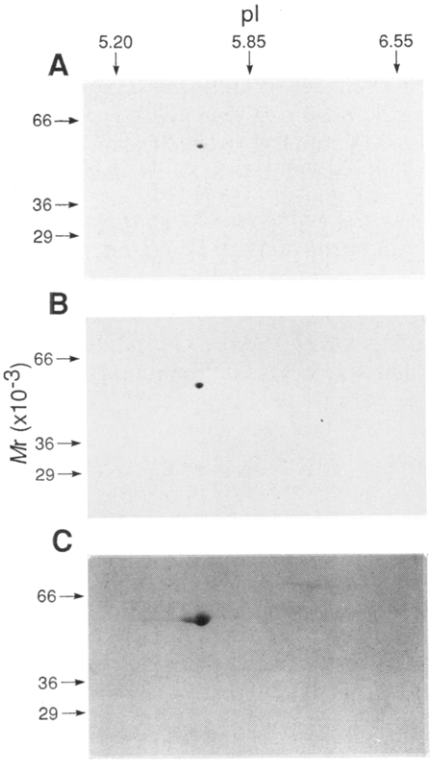

FIGURE 8: Two-dimensional PAGE of rat liver 24K G GDI and bovine brain *smg* p25A GDI. 24K G GDI and *smg* p25A GDI were subjected to two-dimensional PAGE followed by protein staining with silver. (A) 24K G GDI (1 μg of protein); (B) *smg* p25A GDI (1 μg of protein); (C) 24K G GDI (1 μg of protein) plus *smg* p25A GDI (1 μg of protein). The protein markers used for the estimation of molecular weight values were the same as those used in Figure 2. The protein markers used for the determination of p*I* were β-lactoglobulin A (p*I* = 5.20), bovine carbonic anhydrase B (p*I* = 5.85), and human carbonic anhydrase B (p*I* = 6.55).

two-dimensional PAGE either separately or as a mixture. On this PAGE, both proteins showed a single spot at the identical position (Figure 8). The p*I* of both proteins was about pH 5.6.

YMC Pack AP-802 C_4 Column Chromatography. Rat liver 24K G GDI and bovine brain *smg* p25A GDI were subjected

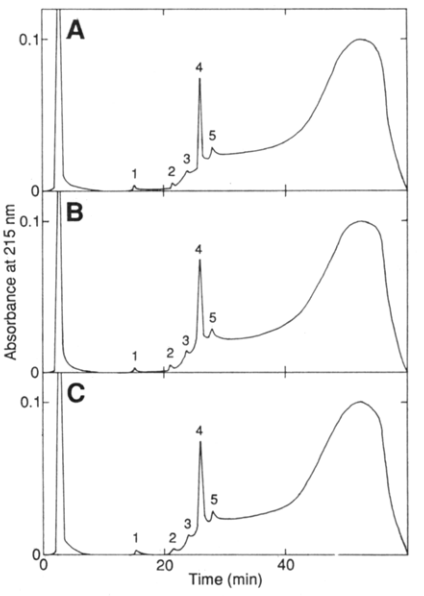

FIGURE 9: YMC pack AP-802 C_4 column chromatography of rat liver 24K G GDI and bovine brain *smg* p25A GDI. 24K G GDI and *smg* p25A GDI were subjected to YMC pack AP-802 C_4 column chromatography. Proteins were detected by measuring the absorbance at 215 nm. (A) 24K G GDI (2 μg of protein); (B) *smg* p25A GDI (2 μg of protein); (C) 24K G GDI (1 μg of protein) plus *smg* p25A GDI (1 μg of protein). Peaks 4 were identified to be 24K G GDI and *smg* p25A GDI by SDS–PAGE. Other peaks were nonprotein contaminants.

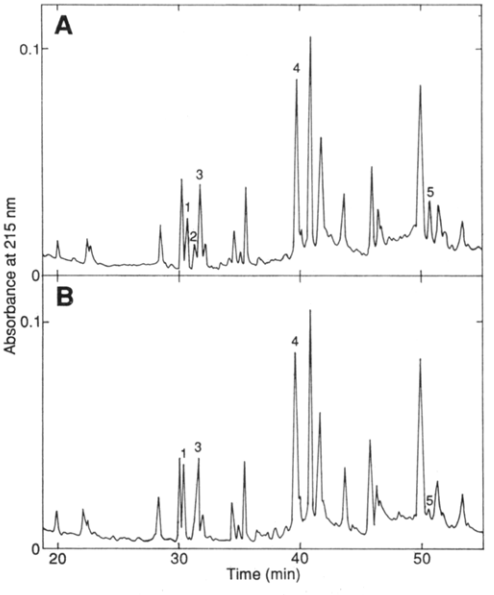

FIGURE 10: Peptide maps of rat liver 24K G GDI and bovine brain *smg* p25A GDI. 24K G GDI and *smg* p25A GDI (13 μg of each protein) were digested with API, and the digested proteins were subjected to Bakerbond WP C_8 column chromatography. Peptide peaks were monitored spectrophotometrically at 215 nm. (A) 24K G GDI; (B) *smg* p25A GDI.

to YMC pack AP-802 C_4 column chromatography either separately or as a mixture. On this column chromatography, both proteins were eluted as a single peak at the same retention time (Figure 9).

Peptide Map and Amino Acid Sequence Analyses. When the purified 24K G GDI and *smg* p25A GDI were completely digested with API and subjected to Bakerbond WP C_8 column chromatography, more than 20 peptides were separated as shown in Figure 10. Most of the peaks were identical for both proteins, but peak 1 of 24K G GDI was smaller than that of *smg* p25A GDI, peak 2 of 24K G GDI was not observed in

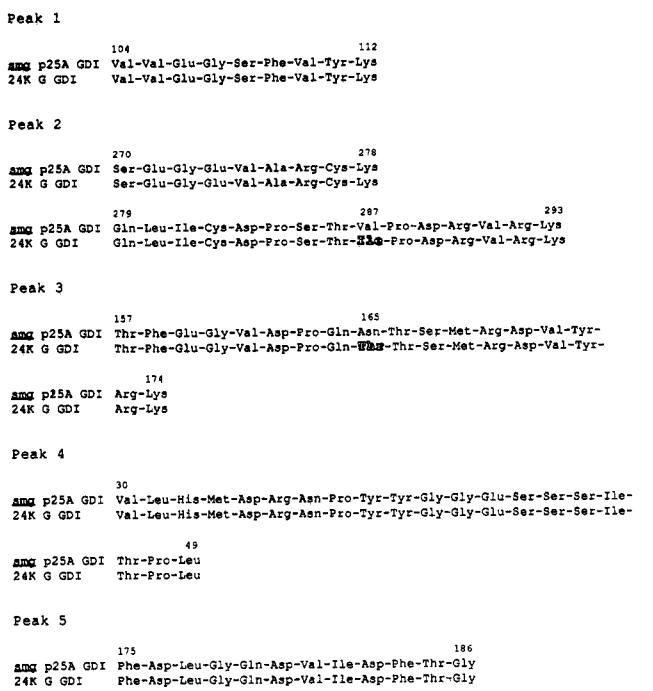

FIGURE 11: Comparison of the amino acid sequences of the peptides of rat liver 24K G GDI with those of bovine brain *smg* p25A GDI. The sequence data of *smg* p25A GDI were taken from Matsui et al. (1990). Peak 2 of 24K G GDI is a mixture of two peptides and corresponds to residues 270–278 and 279–293 of *smg* p25A GDI.

smg p25A GDI, and peak 5 of 24K G GDI was larger than that of *smg* p25A GDI. Five peaks of rat liver 24K G GDI were sequenced by using an automated gas-phase sequencer. Rat liver 24K G GDI had no significant amino acid sequence homology with *rho* GDI but had a high amino acid sequence homology with *smg* p25A GDI. The amino acid sequences of peaks 1–5 of rat liver 24K G GDI were compared with those of bovine brain *smg* p25A GDI in Figure 11. The amino acid sequences of peaks 1, 4, and 5 were identical with those of residues 104–112, 30–49, and 175–186 of *smg* p25A GDI, respectively. The amino acid sequences of peaks 2 and 3 were, however, different from those of *smg* p25A GDI. In peak 2, the 287th residue was Ile, and in peak 3, the 165th residue was Thr for 24K G GDI.

Discussion

In a previous paper, we have purified 24K G to near-homogeneity from the microsomes–Golgi complex fraction of rat liver (Ohmori et al., 1990). 24K G was a novel G protein, not identical with any G proteins described previously. The modes of activation and action of 24K G are not clarified, but we have shown here that the cytosol fraction of rat liver contains a regulatory protein for 24K G. We have recently proposed that small G proteins are regulated by at least three types of regulatory proteins such as GAP, GDI, and GDS (Ueda et al., 1989, 1990; Kikuchi et al., 1989; Ohga et al., 1989; Sasaki et al., 1990; Yamamoto, J., et al., 1990; Yamamoto, T., et al., 1990; Isomura et al., 1990). We have not detected the GAP or GDS activity for 24K G in the cytosol fraction of rat liver. Though these regulatory proteins have been purified from cytosol fractions so far, it is possible that GAP and/or GDS for 24K G are present in other fractions or that they are induced by taking food or some stimulants or certain pathological conditions. We have purified 24K G GDI from the rat liver cytosol fraction to near-homogeneity and characterized its physical and kinetic properties. It is clear that 24K G GDI is a single polypeptide without a subunit structure and regulates the GDP/GTP exchange reaction of 24K G by inhibiting the dissociation of GDP from and the subsequent binding of GTP to it. 24K G GDI is specific for 24K G and inactive for c-Ha-*ras* p21, *rho*B p20, *smg* p21B, and *smg* p25A in inhibiting the dissociation of GDP from and the binding of GTP to each G protein. Moreover, 24K G GDI lacks GAP activity for 24K G, c-Ha-*ras* p21, *rho*B p20, *smg* p21B, and *smg* p25A. Therefore, it is likely that 24K G GDI is different from other regulatory proteins for small G proteins thus far identified, such as GDIs for *smg* p25A and *rho*B p20, GAPs for *ras* p21, *smg* p21s, and the *rho* proteins, and GDSs for *smg* p21s and the *rho* proteins.

We have, however, found that bovine brain *smg* p25A GDI is also active for 24K G. So we have characterized 24K G GDI precisely in comparison with *smg* p25A GDI. We have shown here that *smg* p25A GDI is effective for both 24K G and *smg* p25A but 24K G GDI is effective for only 24K G. The physical properties of 24K G GDI are almost the same as those of *smg* p25A GDI, and the partial amino acid sequences of 24K G GDI revealed that 24K G GDI is highly homologous to *smg* p25A GDI. *smg* p25A GDI mRNA is present in various bovine tissues, including not only the tissues where *smg* p25A and its mRNA are detected but also the tissues where they are not detected in rat (Mizoguchi et al., 1989; Matsui et al., 1990). In bovine liver, the *smg* p25A GDI mRNA is detected, but *smg* p25A and its mRNA are not detected in rat liver. These results have raised the possibility that the G proteins recognized by *smg* p25A GDI other than *smg* p25A may be present in the tissues where *smg* p25A is not detected. Recently, in human platelets we have found a small G protein, similar to but not identical with *smg* p25A, which is recognized by *smg* p25A GDI, and a GDI for this small G protein, similar to *smg* p25A GDI (Fujioka et al., 1990). From the present results together with these earlier observations, it is conceivable that 24K G GDI is the rat liver counterpart of the bovine brain *smg* p25A GDI and that in liver the G protein recognized by *smg* p25A GDI is 24K G. If not the counterpart, it is likely that 24K G GDI is a member of *smg* p25A GDI family.

The reason why 24K G GDI is not effective for *smg* p25A is not known at present. It is possible that the region of 24K G GDI containing at least two different amino acids may interact with *smg* p25A but not with 24K G. It is also possible that the conformational change of 24K G GDI due to at least two different amino acids may make it inactive for *smg* p25A. Mutational analyses by replacement of these different amino acids are necessary to clarify the regions that interact with 24K G and *smg* p25A.

We have previously discussed the role of GDIs in the regulation of the *smg* p25A and *rho* protein activities (Sasaki et al., 1990; Ohga et al., 1989; Ueda et al., 1990). It has been shown that the agonist-bound membrane receptors linked to G proteins serving as transducers and guanine nucleotide exchanging proteins for initiation and elongation factors for protein synthesis stimulate the dissociation of GDP from and the subsequent binding of GTP to the respective G proteins (Ui, 1984; Stryer, 1986; Bourne, 1986; Gilman, 1987; Kaziro, 1978; Pain, 1986). The *CDC25* protein has been also suggested to serve as a stimulatory regulatory protein for the *RAS* protein in yeast (Broek et al., 1987). Since 24K G GDI inhibits the dissociation of GDP from and the subsequent binding of GTP to 24K G, this protein appears to serve as an inhibitory regulatory protein for 24K G and is apparently different from membrane receptors and the *CDC25* protein. If the inhibitory action of 24K G GDI is reversed by covalent

protein modification or by another factor which is regulated by intracellular messengers such as Ca^{2+}–calmodulin, cyclic AMP dependent protein kinase, protein kinase C, and tyrosine kinases, 24K G GDI may exhibit the stimulatory action and regulate the 24K G activity in the same manner as membrane receptors and the *CDC25* protein.

On the other hand, it has been shown that the $\beta\gamma$ subunits of heterotrimeric G proteins bind to the GDP-bound form of the α subunit and thereby inhibit the dissociation of GDP from the α subunit (Gilman, 1987). The property of 24K G GDI as well as *smg* p25A GDI and *rho* GDI is apparently similar to that of the $\beta\gamma$ subunits. 24K G GDI is present in the cytosol, whereas the $\beta\gamma$ subunits attach to membranes. If there is a factor stimulating the dissociation of GDP from 24K G which is analogous to membrane receptors, 24K G GDI could regulate the 24K G activity in the same manner as the $\beta\gamma$ subunits of heterotrimeric G proteins.

Available evidence suggests that the *smg* p25A–*smg* p25A GDI system may be involved in the regulated secretory pathway (Mizoguchi et al., 1989, 1990). The 24K G–24K G GDI system may be involved in the constitutive secretory pathway in liver, but any G proteins functioning at each step in the secretory processes, from ER to Golgi, from one Golgi stack to another, from Golgi to secretory vesicles, and from secretory vesicles to the plasma membrane, have not been apparently identified. If 24K G GDI is the rat liver counterpart of bovine brain *smg* p25A GDI, it is suggested that this GDI is common for the G proteins involved in the secretory processes in both the regulated and the constitutive pathway and that each G protein recognized by this GDI plays an important role at each step in the secretory processes. Since 24K G GDI is isolated from the cytosol fraction of rat liver, it is conceivable that 24K G directly interacts with 24K G GDI at the surface of the ER and/or Golgi complex and operates in a particular step in the secretory pathways. Further investigations are necessary to clarify the functions and modes of action of the 24K G–24K G GDI system in liver.

Acknowledgments

Amino acid sequencing of 24K G GDI was kindly performed by Dr. N. Kubota (Fuji Gotemba Research Laboratories, Chugai Pharmaceutical Co., Ltd., Shizuoka, Japan).

References

Barbacid, M. (1987) *Annu. Rev. Biochem. 56*, 779–827.
Bourne, H. R. (1986) *Nature 321*, 814–816.
Bourne, H. R. (1988) *Cell 53*, 669–671.
Bradford, M. M. (1976) *Anal. Biochem. 72*, 248–254.
Broek, D., Toda, T., Michaeli, T., Levin, L., Birchmeier, C., Zoller, M., Powers, S., & Wigler, M. (1987) *Cell 48*, 789–799.
Burgoyne, R. D. (1987) *Nature 328*, 112–113.
Fujioka, H., Kikuchi, A., Yoshida, Y., Kuroda, S., & Takai, Y. (1990) *Biochem. Biophys. Res. Commun. 168*, 1244–1252.
Fukumoto, Y., Kaibuchi, K., Hori, Y., Fujioka, H., Araki, S., Ueda, T., Kikuchi, A., & Takai, Y. (1990) *Oncogene 5*, 1321–1328.
Garrett, M. D., Self, A. J., Oers, C. V., & Hall, A. (1989) *J. Biol. Chem. 264*, 10–13.
Gibbs, J. B., Schaber, M. D., Allard, W. J., Sigal, I. S., & Scolnick, E. M. (1988) *Proc. Natl. Acad. Sci. U.S.A. 85*, 5026–5030.
Gilman, A. G. (1987) *Annu. Rev. Biochem. 56*, 615–649.
Gomperts, B. D. (1986) *Trends Biochem. Sci. 11*, 290–292.
Goud, B., Salminen, A., Walworth, N. C., & Novick, P. J. (1988) *Cell 53*, 753–768.
Hall, A., & Self, A. J. (1986) *J. Biol. Chem. 261*, 10963–10965.
Hoshino, M., Clanton, D. J., Shih, T. Y., Kawakita, M., & Hattori, S. (1987) *J. Biochem. 102*, 503–511.
Isomura, M., Kaibuchi, K., Yamamoto, T., Kawamura, S., Katayama, M., & Takai, Y. (1990) *Biochem. Biophys. Res. Commun. 169*, 652–659.
Kaziro, Y. (1978) *Biochim. Biophys. Acta 505*, 95–127.
Kikuchi, A., Yamashita, T., Kawata, M., Yamamoto, K., Ikeda, K., Tanimoto, T., & Takai, Y. (1988) *J. Biol. Chem. 263*, 2897–2904.
Kikuchi, A., Sasaki, T., Araki, S., Hata, Y., & Takai, Y. (1989) *J. Biol. Chem. 264*, 9133–9136.
Kim, S., Kikuchi, A., Mizoguchi, A., & Takai, Y. (1989) *Mol. Brain Res. 6*, 167–176.
Kuroda, S., Kikuchi, A., & Takai, Y. (1989) *Biochem. Biophys. Res. Commun. 163*, 674–681.
Laemmli, U. K. (1970) *Nature 227*, 680–685.
Martin, R. G., & Ames, B. N. (1961) *J. Biol. Chem. 236*, 1372–1379.
Matsui, Y., Kikuchi, A., Kondo, J., Hishida, T., Teranishi, Y., & Takai, Y. (1988) *J. Biol. Chem. 263*, 11071–11074.
Matsui, Y., Kikuchi, A., Araki, S., Hata, Y., Kondo, J., Teranishi, Y., & Takai, Y. (1990) *Mol. Cell. Biol. 10*, 4116–4122.
Mizoguchi, A., Kim, S., Ueda, T., & Takai, Y. (1989) *Biochem. Biophys. Res. Commun. 162*, 1438–1445.
Mizoguchi, A., Kim, S., Ueda, T., Kikuchi, A., Yorifuji, H., Hirokawa, N., & Takai, Y. (1990) *J. Biol. Chem. 265*, 11872–11879.
O'Farrell, P. H. (1975) *J. Biol. Chem. 250*, 4007–4021.
Ohga, N., Kikuchi, A., Ueda, T., Yamamoto, J., & Takai, Y. (1989) *Biochem. Biophys. Res. Commun. 163*, 1523–1533.
Ohmori, T., Kikuchi, A., Yamamoto, K., Kim, S., & Takai, Y. (1989) *J. Biol. Chem. 264*, 1877–1881.
Ohmori, T., Takeyama, Y., Ueda, T., Hiroyoshi, M., Nakanishi, H., Ohyanagi, H., Saitoh, Y., & Takai, Y. (1990) *Biochem. Biophys. Res. Commun. 169*, 816–823.
Pain, V. M. (1986) *Biochem. J. 235*, 625–637.
Salminen, A., & Novick, P. J. (1987) *Cell 49*, 527–538.
Sasaki, T., Kikuchi, A., Araki, S., Hata, Y., Isomura, M., Kuroda, S., & Takai, Y. (1990) *J. Biol. Chem. 264*, 2333–2337.
Satoh, T., Nakamura, S., Nakafuku, M., & Kaziro, Y. (1988) *Biochim. Biophys. Acta 949*, 97–109.
Segev, N., Mulholland, J., & Botstein, D. (1988) *Cell 52*, 915–924.
Shoji, I., Kikuchi, A., Kuroda, S., & Takai, Y. (1989) *Biochem. Biophys. Res. Commun. 162*, 273–281.
Stryer, L. (1986) *Annu. Rev. Neurosci. 5*, 277–279.
Takai, Y., Kikuchi, A., Yamashita, T., Yamamoto, K., Kawata, M., & Hoshijima, M. (1988) in *Progress in Endocrinology* (Imura, H., Shizume, K., & Yoshida, S., Eds.) Vol. 2, pp 995–1000, Elsevier Science Publishers B.V., Amsterdam, The Netherlands.
Trahey, M., & McCormick, F. (1987) *Science 238*, 542–545.
Trahey, M., Wong, G., Halenbeck, R., Rubinfeld, B., Martin, G. A., Ladner, M., Long, C. M., Crosier, W. J., Watt, K., Koths, K., & McCormick, F. (1988) *Science 242*, 1697–1700.
Ueda, T., Kikuchi, A., Ohga, N., Yamamoto, J., & Takai, Y. (1989) *Biochem. Biophys. Res. Commun. 159*, 1411–1419.

Ueda, T., Kikuchi, A., Ohga, N., Yamamoto, J., & Takai, Y. (1990) *J. Biol. Chem. 265*, 9373-9380.
Ui, M. (1984) *Trends Pharmacol. Sci. 5*, 277-279.
Vogel, U. S., Dixon, R. A. F., Schaber, M. D., Diehl, R. E., Marshall, M. S., Scolnick, E. M., Sigal, I. S., & Gibbs, J. B. (1988) *Nature 335*, 90-93.
West, M., Kung, H., & Kamata, T. (1990) *FEBS Lett. 259*, 245-248.
Wolfman, A., & Macara, L. G. (1990) *Science 248*, 67-69.
Yamamoto, J., Kikuchi, A., Ueda, T., Ohga, N., & Takai, Y. (1990) *Mol. Brain Res. 8*, 105-111.
Yamamoto, K., Kondo, J., Hishida, T., Teranishi, Y., & Takai, Y. (1988) *J. Biol. Chem. 263*, 9926-9932.
Yamamoto, T., Kaibuchi, K., Mizuno, T., Hiroyoshi, M., Shirataki, H., & Takai, Y. (1990) *J. Biol. Chem. 265*, 16626-16634.
Zahraoui, A., Touchot, N., Chardin, P., & Tavitian, A. (1988) *Nucleic Acids Res. 16*, 1204.

X-ray Structure of an Unusual Ca^{2+} Site and the Roles of Zn^{2+} and Ca^{2+} in the Assembly, Stability, and Storage of the Insulin Hexamer†

Christopher P. Hill,‡,§ Zbigniew Dauter,‡,∥ Eleanor J. Dodson,‡ Guy G. Dodson,*,‡ and Michael F. Dunn*,⊥
Department of Chemistry, University of York, Heslington, York YO1 5DD, U.K., and Department of Biochemistry, University of California, Riverside, California 92521-0129

Received July 9, 1990; Revised Manuscript Received September 26, 1990

ABSTRACT: Metal ion binding to the insulin hexamer has been investigated by crystallographic analysis. Cadmium, lead, and metal-free hexamers have been refined to *R* values of 0.181, 0.172, and 0.172, against data of 1.9-, 2.5-, and 2.5-Å resolution, respectively. These structures have been compared with each other and with the isomorphous two-zinc insulin. The structure of the metal-free hexamer shows that the His(B10) imidazole rings are arranged in a preformed site that binds a water molecule and is poised for Zn^{2+} coordination. The structure of the cadmium derivative shows that the binding of Cd^{2+} at the center of the hexamer is unusual. There are three symmetry-related sites located within 2.7 Å of each other, and this position is evidently one-third occupied. It is also shown that the coordinating B13 glutamate side chains of this derivative have two partially occupied conformations. One of these conformations is two-thirds occupied and is very similar to that seen in two-zinc insulin. The other, one-third-occupied conformation, is seen to coordinate the one-third-occupied metal ion. The binding of Ca^{2+} to insulin is assumed to be essentially identical with that of Cd^{2+}. Thus, we conclude that the Ca^{2+} binding site in the insulin hexamer is unlike that of any other known calcium binding protein. The crystal structures reported herein explain how binding of metal ions stabilizes the insulin hexamer. The role of metal ions in hexamer assembly and dissociation is discussed.

When free of divalent metal ions, the protein hormone insulin exists in solution as an equilibrating mixture of monomer, dimer, tetramer, hexamer, and higher aggregates. The hexamer has been shown to contain two high-affinity binding sites for Zn^{2+}, and in the presence of this ion, the distribution of insulin species in solution is driven toward the hexamer state. A wide variety of divalent metal ions will substitute for Zn^{2+} at these sites (Blundell et al., 1972).

Insulin storage vesicles are known to contain high concentrations of Ca^{2+} and Zn^{2+} ions (Howell et al., 1975), and there is evidence that Ca^{2+} is taken up by rhombohedral zinc insulin crystals in vivo (Howell et al., 1978). From the available in vivo evidence, it appears likely that Ca^{2+} interactions with the zinc proinsulin and zinc insulin hexamers are important and that the form of insulin within mature storage vesicles is crystalline (Greider et al., 1969). The three-dimensional structure of the two-zinc insulin hexamer, $(In)_6(Zn^{2+})_2$,[1] has been solved to a resolution of 1.5 Å (Baker et al., 1988). The hexamer is a torus-shaped molecule with dimensions 35 Å by 50 Å (Figure 1). The six insulin subunits are arranged as a trimer of asymmetric dimers about a 3-fold symmetry axis. The two high-affinity zinc sites are located on the 3-fold axis separated by a distance of 15.9 Å. Each site is formed by three His(B10) imidazole ligands (one from each dimer) as shown in Figure 2; octahedral coordination at each site is completed by water molecules.

The work of Schlichtkrull (1956) on the stoichiometries of divalent metal ion binding in crystalline rhombohedral insulin hexamers gave the first indication of the presence of a third, high-affinity metal ion binding site within the insulin hexamer. During the determination of the structure of $(In)_6(Zn^{2+})_2$, isomorphous replacement studies with Cd^{2+}, Pb^{2+}, and UO_2^{2+} ions indicated the presence of a metal binding site in the vicinity of the center of the hexamer (Adams et al., 1967; Blundell et al., 1972). The X-ray diffraction study of Emdin et al. (1980) showed that when crystals of $(In)_6(Zn^{2+})_2$ were soaked in solutions containing high concentrations of Zn^{2+}, the crystals bind Zn^{2+} at a variety of sites, including the

† Supported by NIH Grants AM31138 BMT and DK42124, the American Diabetes Association, the Kroc Foundation, the Medical Research Council, and the Science and Engineering Research Council.
‡ University of York.
§ Present address: Molecular Biology Institute and Department of Chemistry and Biochemistry, University of California, Los Angeles, CA 900245-1569.
∥ Present address: EMBL, Notkestrasse 85, 2000 Hamburg, FRG.
⊥ University of California, Riverside.

[1] Abbreviations: NMR, nuclear magnetic resonance; FT, Fourier transform; $(In)_6(M^{2+})_m(M^{2+})_n$, metal-substituted insulin hexamers where *m* and *n* designate the stoichiometries of metal ions bound to the His(B10) and Glu(B13) sites, respectively; $(In)_6$, metal-free insulin hexamer.

0006-2960/91/0430-917$02.50/0